Biochimica et Biophysica Acta 1838 (2014) 1793–1800

Contents lists available at ScienceDirect

Biochimica et Biophysica Acta

journal homepage: www.elsevier.com/locate/bbamem

Evaluations of a mechanistic hypothesis for the influence of extracellular ions on electroporation due to high-intensity, nanosecond pulsing

V. Sridhara [a], R.P. Joshi [b,*]

[a] Center for Computational Biology and Bioinformatics, College of Natural Sciences, University of Texas, 2415 Speedway, C4500, Austin, TX 78712, United States
[b] Dept. of Electrical & Computer Engineering and Frank Reidy Center for Bio-Electrics, Old Dominion University, Norfolk, VA 23529-0246, United States

ARTICLE INFO

Article history:
Received 27 November 2013
Received in revised form 17 March 2014
Accepted 18 March 2014
Available online 26 March 2014

Keywords:
Nanopore
Ions
Lipid
Molecular dynamics
Electric pulsing

ABSTRACT

The effect of ions present in the extracellular medium on electroporation by high-intensity, short-duration pulsing is studied through molecular dynamic simulations. Our simulation results indicate that mobile ions in the medium might play a role in creating stronger local electric fields across membranes that then reinforce and strengthen electroporation. Much faster pore formation is predicted in higher conductivity media. However, the impact of extracellular conductivity on cellular inflows, which depend on transport processes such as electrophoresis, could be different as discussed here. Our simulation results also show that interactions between cations (Na^+ in this case) and the carbonyl oxygen of the lipid headgroups could impede pore resealing.

1. Introduction

The effect of intense pulsed electric fields on biological cells and tissues has been the topic of research since the late 1950s, with the first report of electric-field assisted reversible breakdown of cell membranes by R. Stampfli [1]. The orders of magnitude increase in plasma membrane permeability of a biological cell were termed "electroporation" [2]. Electroporation involves [1,3,4] rapid structural rearrangement of the membrane, leading to the rapid increase of electrical conductivity [5] associated with the formation of pores in the lipid bilayer. The existence of pores has not been experimentally verified in a unique and unambiguous manner. Here, pores are taken to denote some kind of highly conductive pathways created in the membrane due to an externally applied electric field that increase membrane conductivity. Furthermore, these pores facilitate the uptake and flow of molecules and ions. Electroporation can, therefore, be used to initiate molecular fluxes for purposes of introducing a genetic material into cells, and numerous other applications [6–10]. Besides membrane electroporation [11–14], high-intensity, short-duration (HISD) electrical pulses have been shown to promote electrically-triggered intra-cellular calcium release [15–17], the destruction of micro-organisms [11,18], and killing of tumor cells [11,19], and bring about DNA damage [20]. Typical pore diameters upon electroporation with HISD pulsing have been predicted to be on the order of 1.6 nm with about a 0.6 nm statistical spread [12,13,21–25], and roughly verified by tracking transport of fluorescent dyes through cell membranes [11].

Multiple experimental studies have demonstrated that the extracellular medium conductivity (σ_e) has an influence on the electroporation phenomenon [26–30]. Though these studies were not conducted under HISD conditions, they do probe the overall conductivity trend of the same physical phenomena (i.e. electroporation). In this context, it may be mentioned that in the above studies, the depletion of ions from the medium was osmotically counterbalanced with neutral compounds such as sucrose. Hence osmolarity was not a factor in influencing the electroporation results. In addition, the decreased rates in poration efficiency observed with reduced conductivity were reported to be higher for lower medium conductivity (σ_e) values. A hypothesis that has been proposed for explaining this σ_e dependence is that the induced transmembrane potential (TMP) depends on the conductivity of the extracellular medium [31]. This is based on the notion that voltage drops across heterogeneous segments depend on the local conductivities. Since the threshold for electroporation can only be reached if the requisite TMP values are attained, this is more easily achievable at higher values of σ_e which supports a higher membrane voltage drop. With high extracellular medium conductivities, a larger fraction of the applied potential would be developed across the cell membrane and its intracellular region, thus forcing larger electroporation and ion flows.

The situation with regards to the effect of ionic strength on electroporation may seemingly appear somewhat murky. An early report by Rols and Teissie [32] indicated that in higher ionic strength mediums, permeabilization was enhanced and polyethylene glycol (PEG) molecules of a

Abbreviations: MD, molecular dynamics; DPPC, dipalmitoylphosphatidylcholine; TMP, transmembrane potential

* Corresponding author.
E-mail address: rjoshi@odu.edu (R.P. Joshi).

http://dx.doi.org/10.1016/j.bbamem.2014.03.010
0005-2736/

higher molecular mass were required in the extracellular medium to block the entry of Trypan Blue in Chinese hamster ovary cells. A similar conclusion was reported more recently [33], wherein decreases in medium conductivity made it necessary to deliver electric pulses of larger amplitude in order to achieve the same electroporative effect. The studies by Suzuki et al. [34] again suggested the stronger role on electroporation arising from a higher medium conductivity (e.g., Fig. 8 in their referenced report). For example, the change in the electroporated cell membrane conductance in low conductivity medium was observed to be much smaller. However, a recent report by Li et al. [35] probed transport of ions and the inflow of propidium iodide through porated membranes on the extracellular conductivity based on a coupled Nernst–Planck, Smoluchowski approach. Their theory and results indicate that the transport of the ions or molecular delivery into cells has the form: $3\sigma_i/(2\sigma_e + \sigma_i)$, where $\sigma_{i,e}$ are the conductivities of the intra- and extra-cellular media, respectively. Hence, a higher extracellular conductivity (σ_e) would suggest a lower molecular delivery into the cell. This apparent discrepancy is easily resolved once it is realized that these various studies are essentially *probing two separate aspects*. The throughput or inflow into cells depends on transport phenomena such as electrophoresis, while poration is simply the initial stage of cell membrane opening that then sets into motion the downstream event of an inflow. These aspects are further discussed later in the manuscript and any seeming discrepancies resolved.

A relatively recent study [36] shows that transient water pores can be induced across a cell membrane by charge imbalance. These pores have been predicted to form quickly on nanosecond time scales based on molecular dynamic simulations. Under equilibrium conditions in cellular membranes, the TMP values typically correspond to the average ion concentration gradients which are sufficient to create voltage differences on the order of 100 mV across the membrane. However, in the presence of a high-intensity external electric field (~100 kV/cm), localized charge movements may presumably occur leading to the creation of large perturbations in the local electric fields. Thus, the total driving force seen by the membrane lipid chains could conceivably be altered by the presence of mobile ions in the solvent, thereby creating a natural dependence of medium conductivity on electroporation.

We focus on the effects of medium conductivity on electroporation in response to high intensity (~100 kV/cm), ultrashort (~10–20 ns) pulsing. Experimental studies of TMP generation and electroporation due to such nanosecond pulsing have been reported [37]. In these situations the times scales are very short, and subsequently downstream processes such as cell swelling due to unequal flows of ions and molecules across the cell membrane [38,39], are irrelevant and play no role. We hypothesis that mobile ions in the medium play a role in creating stronger local electric fields across membranes that then reinforce and strengthen the electroporation process. Our simulation results will also show that interactions between cations (Na^+ in this case) and the carbonyl oxygen of the lipid headgroups can form complexes that likely impede pore resealing. Hence, the long-lived pores that have recently been observed in the context of high-intensity, nanosecond pulsing [40] could well be a manifestation of such interactions.

2. Methods and model

The dynamics of pore formation in lipid cell membranes in response to an externally applied electric field, in the presence of ions near the membrane are studied based on molecular dynamic (MD) simulations performed using GROMACS [41]. For accuracy, a small 2 fs time step has been used. Typically, MD simulations in such situations are carried out by selecting a segment of the lipid bilayer membrane and constructing initial geometric arrangement of all the atoms and their bonding angles. Here dipalmitoylphosphatidylcholine (DPPC) lipids were used for the membrane. We used a DPPC bilayer consisting of 128 lipids with and without ions to evaluate whether ionic gradients might aid in the pore formation process. Na^+ and Cl^- ions were used in the extracellular water. Regions of water are then defined on either side of the membrane to form the total simulation space. The SPC model was used for the water molecules. The electric field was applied in a direction perpendicular to the bilayer–water interface (the *z*-direction). The force field parameters were taken from the united atom field of Berger et al. [42]. Simulations were at constant particle number and temperature (300 K), using a Berendsen thermostat [43] with a coupling time constant of 0.1 ps for DPPC and water. Our choice was based on conditions that are more in tune with many of the experiments conducted, which have been around room temperature. At this temperature chosen, the DPPC would be in the gel phase since the phase transition of DPPC occurs around 314.4 K [44–46]. Our relatively low temperature of 300 K represents a "worst-case conservative" scenario in a way. The lower temperature would, if anything, actually increase the electric field strength required for membrane poration due to the higher membrane rigidity. On the other hand, the effects of electrostatic interactions, both from the external electric field and due to the ions in the vicinity of the membrane, would be stronger at a higher temperature. Furthermore, Ziegler and Vernier [47] demonstrated that the minimum porating electric field showed no correlation in simulations carried out for temperatures between 280 K and 340 K. While some of the quantitative details concerning electroporation and the membrane response could change at a different temperature, the qualitative trends would remain. Semi-isotropic weak pressure coupling (compressibility 4.5×10^{-5} bar^{-1}, time constant 1 ps) was employed in the lateral direction with pressure set to 1 bar in the *x*–*y* direction, with no pressure coupling in the *z*-direction (normal to the water–DPPC interface). Long-range electrostatic interactions were computed with a particle mesh Ewald (PME) method [48] with a cutoff radius of 1 nm and a grid of 0.15 nm. Periodic boundary conditions were used to keep the particles within the simulation region as is usually done in MD work. A 1 nm cut-off was used for the van der Waals interactions. A 0.9/1.2 nm group based twin cutoff scheme was employed for the Lennard–Jones interactions. The linear constraint solver (LINCS order 4) algorithm outlined by Hess et al. [49] was used to constrain all the bond lengths within the lipids and on the water geometry.

For the system without any ions, there were 9376 water molecules resulting in a total of 34,528 atoms in the system. Each DPPC molecule consisted of 50 atoms in an all-atom model. The total size of the overall simulated system was 6.36 nm × 6.38 nm × 10.59 nm. This chosen volumetric geometry implies that 1 ion placed inside such a simulation region roughly corresponds to a ~3.8 mM system. Though a fairly high density, the MD simulations used here serve as an accelerated numerical test to probe the potential role of ions present in the external medium on pore formation. More realistic and lower concentrations would have required much larger simulation times, and the overall process would have become almost intractable given that multiple trials have to be performed to obtain reliable statistical results. The biophysics and the qualitative trends obtained here, however, are expected to be qualitatively correct. As is well known, the MD technique for any given simulation scenario can yield results that depend on the initial values assigned, specifically the molecular velocities. Here for statistical significance, a total of six MD simulations were carried out with different starting molecular velocities for the various conditions simulated and discussed in the next section. The results shown in the next section represent typical simulation outcomes. Plots of the trajectories and atomic configurations were obtained by using visual molecular dynamics (VMD) [50].

3. Results and discussion

The effects of ions in close proximity to a cell membrane on electroporation were explored through MD simulations. Several different simulations were carried out in which both the external electric field strength and the number of ions present in the simulation system were varied in different ways. The first set of simulations used 2 Na^+ and 2 Cl^- ions on each side of the DPPC membrane at an electric field of 0.45 V/nm. The starting structure is shown in Fig. 1a with the yellow circles

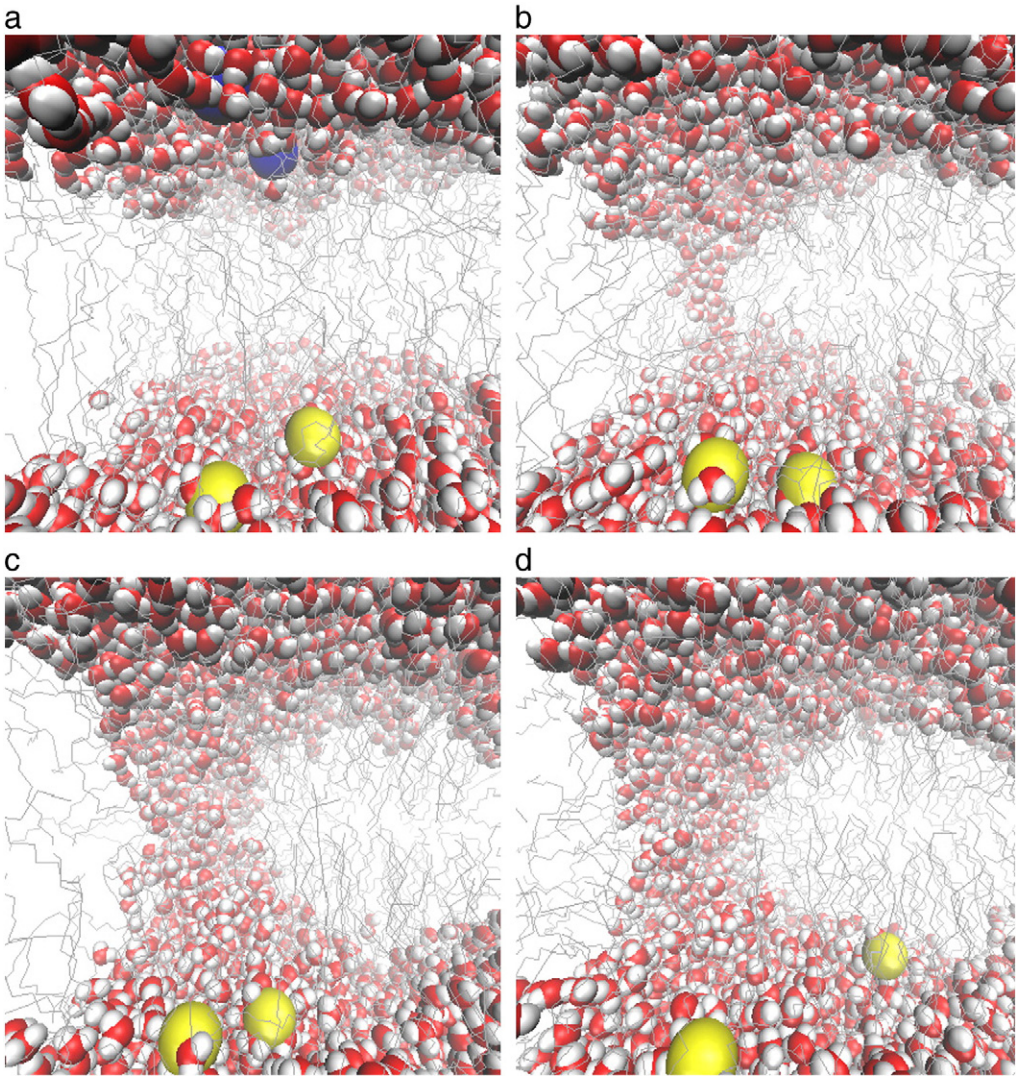

Fig. 1. MD simulations showing synergistic effects of ionic gradients ($2Na^+/2Cl^-$ ions) and ultra-short electrical pulses (0.45 V/nm for 20 ns) on a DPPC bilayer. (a) Starting structure of the DPPC bilayer with 2 Na^+ and 2 Cl^- ions. For clarity, DPPC molecules are shown as thin wires, while Na^+ and Cl^- ions are shown by yellow and blue circles, respectively. Water molecules are shown in red-and-grey colors. Only 1 Cl^- ion is visible in the figure. (b) The system at 1.5 ns, where water wires seem to result in pore initiation. (c) Snapshot at 4 ns, showing a stable pore formation. (d) System at the end of the 20 ns pulse. As evident 1 Na^+ ion appears to be trapped at the membrane–water interface region, while the 2nd Na^+ ion stays within the membrane–water interface region throughout the entire simulation run.

representing the Na^+ ions, while Cl^- ions are shown in blue. Fig. 1b shows a snapshot of the system at 1.5 ns, a time instant when the pore just starts to form. At 4 ns, a stable pore seems to be in place as seen in Fig. 1c. The final structure of the system at 20 ns is shown in Fig. 1d. An interesting feature observed in this simulation is that the Na^+ ions seems to lie near the lipid headgroups and spends considerable time in this vicinity. This kind of behavior (which is similar to trapping in some way) has been reported in the literature [51,52]. In the case of Na^+, the cations can bind to sites such as the carbonyl oxygen atoms of the headgroup. The forces which give rise to binding involve interactions with the most polar regions of the headgroups. An average of 3 cations reportedly interact [52] leading to large complexes with reduced mobility for Na^+. In theory, the hydrogen ions present in the water (as H_3O^+) can also bind with the lipids in a similar manner and hydrate the headgroups. Such binding thus occurs at the outer leaflet.

In order to investigate the effects without ionic gradient, a separate 20 ns simulation was performed at the same electric field of 0.45 V/nm *but without any ions*. Fig. 2a shows the starting structure, which is similar to Fig. 1a. In this case, no signs of pore formation were seen at 10 ns for this system without ions (Fig. 2b). Even after 15 ns, no pore or water-wire was observed from the simulations. However, a few water molecules did begin to pass through the lipid bilayer and a pore initiation was observed at 15.5 ns as shown in Fig. 2c. Finally at 20 ns, a stable pore appears as seen in Fig. 2d. Clearly from these results, ions seem to play a very important role in the pore formation and significantly enhance the poration rate.

Next, we studied the role of ions in resealing. To understand the resealing effect, we carried out two more simulations, one with and the other without any ions. For the first of the two simulations, a membrane with a pore together with ions in the system was selected as the starting structure. MD simulations for this system were carried out for 20 ns, without any external electric field, for initial stabilization. Fig. 3a shows the starting structure. DPPC molecules are shown as thin wiry chains, water molecules are shown in red-and-grey, Na^+ ions are shown as yellow spheres, while the Cl^- ions are shown in blue. The system after 1 ns (Fig. 3b) shows the pore to be slightly constricted. After around 5 ns, the constriction process appears to slow down, as seen in Fig. 3c. At the end of the 20 ns simulation in Fig. 3(d), the pore is seen to have grown slightly after the initial constriction, although the size is not larger than its initial level of Fig. 3a. The pore size can be gauged by a manual inspection, or more rigorously by keeping track of the number of water molecules within the course of the

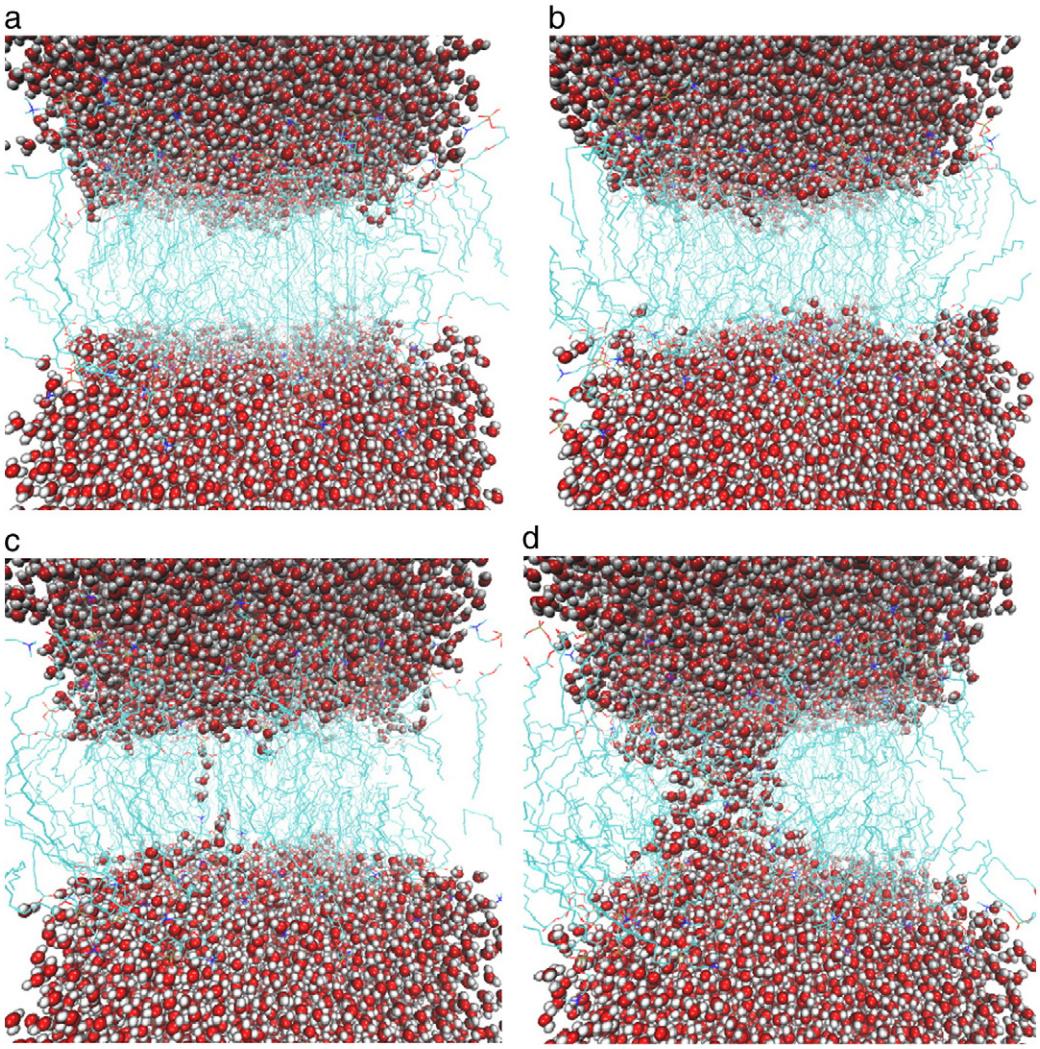

Fig. 2. MD simulation results showing pore formation at 0.45 V/nm in a DPPC bilayer, with no ions in the system. DPPC molecules are shown as thin wires and water molecules are shown in red-and-grey colors. (a) Starting structure of the DPPC bilayer. (b) System at 10 ns, with no signs of pore formation. (c) A 15.5 ns snapshot showing a pore starting to form. (d) Finally, a stable pore appears to have formed at the end of 20 ns duration.

simulation over any specific chosen volume. The qualitative trends are similar for both approaches. The ionic gradient thus seems to play a role in keeping the pore at a somewhat wide level during the resealing process. The alternate scenario of pore resealing without any ions present in the system was next probed by MD simulations. The same starting structure of Fig. 3a was used but with the Na^+ and Cl^- ions removed from the system. Snapshots after 1 ns and 5 ns, shown in Figs. 4b and 4c, respectively, indicate a slight pore constriction. The situation after 20 ns without any ions is shown in Fig. 4(d), and reveals a size to be almost that at the end of 5 ns. Differences in pore sizes between Figs. 3d and 4d are not very obvious and apparent. However manual inspection shows that the pore is slightly larger with ions. More specifically, the number of water molecules for Fig. 3c was 631, while the number of water molecules within the pore for Fig. 4d was slightly smaller at 613. Furthermore, there is a slightly larger constriction in the middle of the pore in Fig. 4d (without ions) than in Fig. 3d. Though the difference is almost insignificant, a smaller number of water molecules were always obtained in our simulations without an ionic gradient.

The above results can be understood in terms of the on-going molecular interactions between the lipid headgroups and the ions. For instance, interactions between sodium ions and the carbonyl oxygen of the lipid headgroups would form complexes binding the hydrophobic and hydrophilic regions of the membrane. This effective connectivity within the membrane would likely impede pore resealing. Furthermore, over time the H_3O^+ cations present in the water would tend to bind to the carbonyl groups in much the same way as the Na^+ ions. This binding would lead to increased molecular densities of water within the pore, a result that exhibits itself in our simulations as the pore size enhancement with a higher water density as seen in Fig. 3(d). On the other hand, with the absence of the binding Na^+ cations, there is no particular formation of rigid lipidic complexes. The natural relaxation and shrinkage of the pore then proceed more naturally as might be expected. The process of water expulsion and pore closure though is slow since energy is required to drive the water out, and provided in part by the stored energy of the deformed membrane.

Finally for concreteness, the movement of ions during the poration process and interactions between ions and the lipid bilayer molecules was probed more fully. In the set of snapshots shown in Fig. 1, the passage of Cl^- ions is not clearly seen. Fig. 5 focusses more on this ionic transport aspect. The Na^+ and Cl^- ions are on either side of the bilayer, with a 0.45 V/nm external electric field applied at the start (Fig. 5a). The system at 4 ns shows the Cl^- ion starting to drift through the pore in Fig. 5(b). The 6 ns snapshot shown in Fig. 5(c) reveals the Cl^- ion drifting to the other side of the pore, and finally exiting the membrane onto the other side at 7 ns. During these various times however, the Na^+ ions are seen to remain at the membrane–water interface region. The strong interactive binding is obvious, and can overcome the strong driving force from the external electric field.

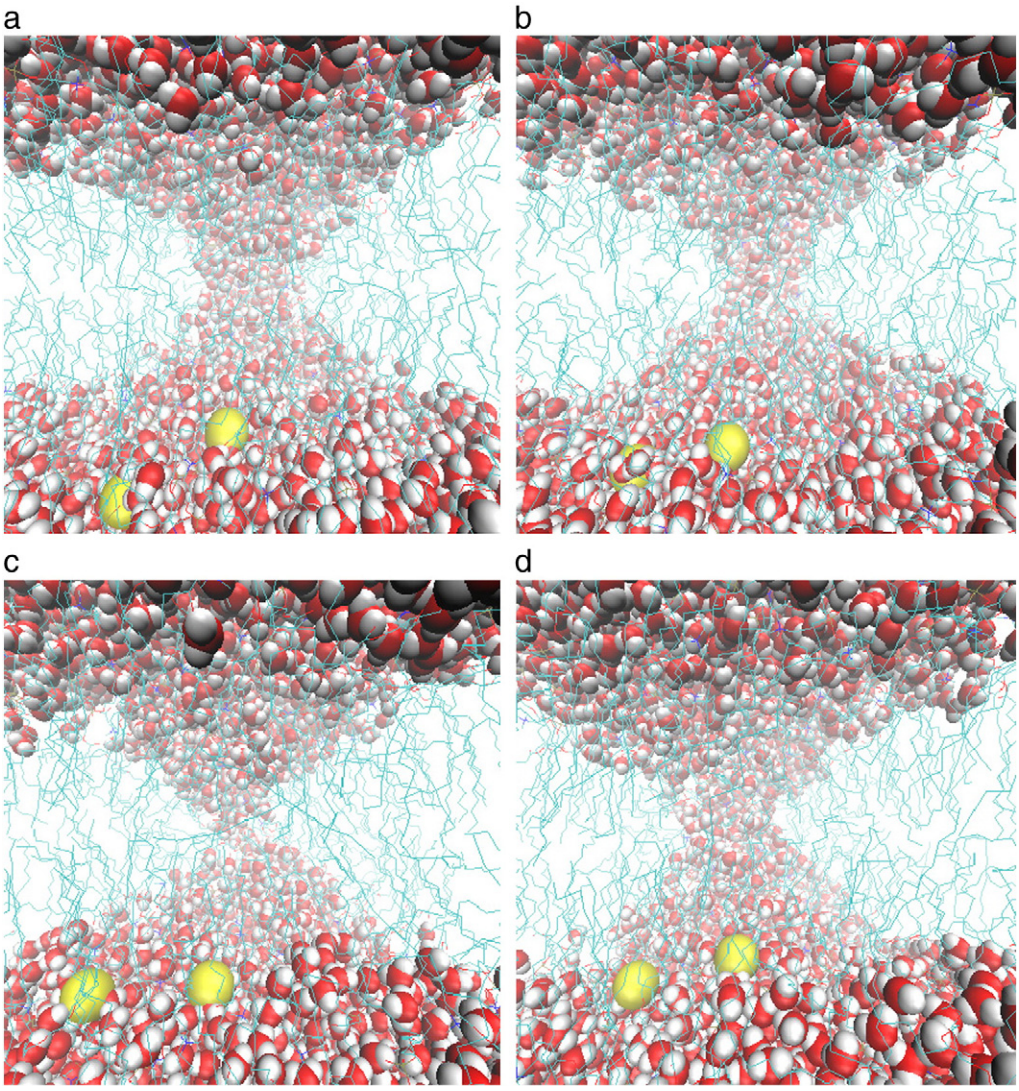

Fig. 3. Role of ionic gradients during the resealing process. DPPC molecules are shown as wiry chains, water molecules are shown in red-and-grey, Na^+ ions are shown as yellow circles, while the Cl^- ions in blue circles are not seen in these views. (a) The bilayer system, starting with the pore obtained from the 0.45 V/nm simulation run with the 2 Na^+ and 2 Cl^- ions. (b) System after 1 ns, with the pore seen to be slightly constricted. (c) At 5 ns, the constriction process appears to slow down. (d) System after 20 ns, with the pore having grown slightly after the initial constriction, although the size is not larger than its initial level. The ionic gradient seems to play a role in keeping the pore slightly wider during the resealing process.

These results also show the relatively weak binding of Cl^- with the lipid molecules. The strong binding for Na^+ is likely to lead to desolvation and loss of its layers of water hydration, with possible injection into the membrane pore region.

As a final point of discussion, we revisit the apparent discrepancy arising from the report by Lin et al. [35]. Their study probed transport of ions and the inflow of propidium iodide through porated membranes on the extracellular conductivity based on a coupled Nernst–Planck, Smoluchowski approach. Their theory and results indicate that the transport of the ions or molecular delivery into cells has the form: $3\sigma_i/(2\sigma_e + \sigma_i)$, where $\sigma_{i,e}$ are the conductivities of the intra- and extra-cellular media. Hence, a higher extracellular conductivity (σ_e) would suggest a lower molecular delivery into the cell. This apparent discrepancy is easily resolved once it is realized that these various studies are essentially *probing two separate aspects*. The throughput or inflow into cells depends on transport phenomena such as electrophoresis, while poration is simply the initial stage of cell membrane opening that then sets into motion the downstream event of an inflow. Our contention is that both the pore area density (i.e. degree of electroporation) and membrane conductance *will increase with higher extracellular conductivity*. In fact, this is also the exact conclusion reached by the same group of Lin et al. [53] in a very recent report based on the continuum theory. There is, thus no discrepancy. The molecular throughput or flow, however, does depend inversely on the extracellular conductivity, but this is not the focus of the present analysis.

A point for completeness, in the above regard is that the analysis by Lin et al. [35,53] omitted the Navier–Stokes equations for the hydrodynamic fluid fields which can also influence ionic translocation. Consideration of the fluid flow (via the Navier–Stokes equations) is important because application of an external electric field drives the ions in the solution, which in turn, drag the surrounding fluid. This electrokinetic manifestation of viscous drag is referred to as electroosmosis. In the nanopore transport case considered here, there would be two distinct types of movements: (a) Electrophoretic migration of ions in response to an electric field, and (b) an electroosmotic flow (EOF) which is the movement of the solvent due to the viscous drag from the flowing ions. The major distinction between these two types of transport is that cations and anions move in different directions in electrophoretic migration, whereas EOF results in bulk fluid movement due to the dominant motion of the ionic species having the greatest mobility and concentration. Furthermore, since EOF is induced by the movement of ions, it tends to collapse in pores for which the electric double layers overlap significantly. In any case, a full discussion and evaluations of ionic flow are beyond the present scope.

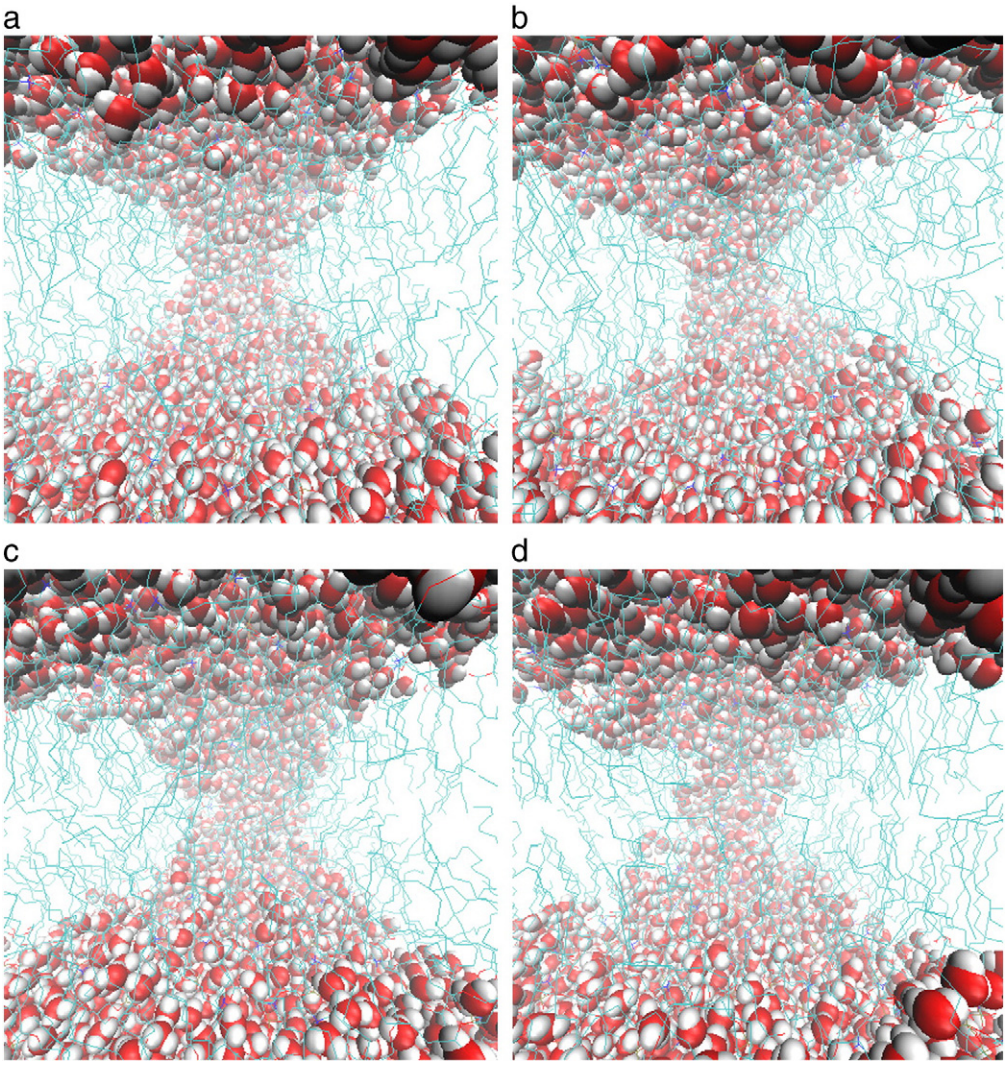

Fig. 4. MD simulations of the resealing process without ionic gradients. (a) The same starting structure as shown in Fig. 3a, but with the Na^+ and Cl^- ions removed from the structure. (b) System at 1 ns showing a slight pore constriction. (c) A 5 ns snapshot where the constriction process slows somewhat similar to the case with ionic gradients. (d) Resealing after 20 ns, with the pore appearing to remain at about the same size as in Fig. 4c without any enlargement.

A few final comments are perhaps in order. First, sodium ions are not unique, but were chosen here simply since they represent a common example of an extracellular ion. Others such as Ca^{2+} could also have been probed, but we believe that the additional additive contribution from the electrostatics standpoint to electroporation would remain. However, the use of different ions could in theory be a separate interesting study to probe differences in electroporation rates or magnitudes. Additional simulations could be done to confirm the effect of ions on the membrane with specific experiments, including the role of ions in mediated throughput into cells. The general agreement with the numerous studies cited here (e.g., Refs. 26–30, 32–35, 49) does support the present thesis. Second, the exact membrane response and details surrounding the electroporation dynamics could change at a higher temperature for which the membrane is not in the gel phase. However, the underlying physics and the qualitative trends would likely remain. Finally, it might be mentioned that the details of the poration dynamics could also depend on the properties (such as the dipole potential) of the membrane and the components of its hydrophobic tails [54]. For instance, as shown recently by Polak et al. [54], dipalmitoylphosphatidylcholine (DPPC), diphytanoyl-phosphocholine-ester (DPhPC-ester), and diphytanoyl-phosphocholine-ether (DPhPC-ether) based bilayers showed differences in the electroporation thresholds.

4. Conclusions

In summary, the effect of ions present in the extracellular medium on electroporation by high-intensity, short-duration pulsing was studied through MD simulations. Over the short time scales, eventual downstream processes such as cell swelling and unequal flows of ions and molecules across the cell membrane would be irrelevant. Though not exhaustive, our simulation results do suggest that mobile ions in the medium play a role in creating stronger local electric fields across membranes that then reinforce and strengthen the electroporation process. Much faster pore formation is predicted to be another outcome in higher conductivity media. Our simulation results also show that interactions between cations (Na^+ in this case) and the carbonyl oxygen of the lipid headgroups can form complexes that likely impede pore resealing. Hence, the long-lived pores that have recently been observed in the context of high-intensity, nanosecond pulsing [40] could well be a manifestation of such interactions.

Disclosure

The authors report no conflicts of interest in this study.

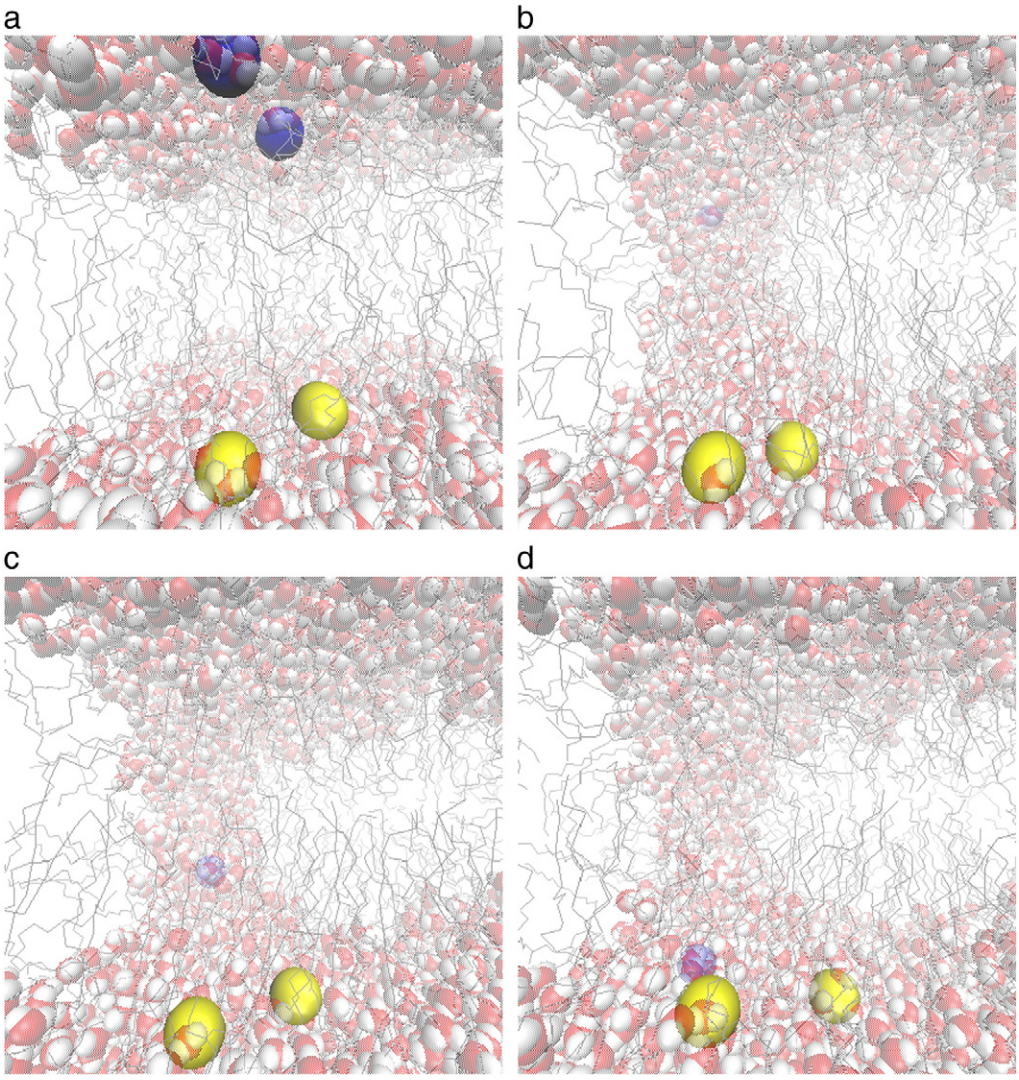

Fig. 5. Electrical field effects on Na^+ and Cl^- ions during nanopore formation. These snapshots are for the same run as Fig. 1, but focus on the Na^+ and Cl^- ion movements during. (a) The starting structure of the bilayer system at 0 ns. An electrical field of 0.45 V/nm was applied for 20 ns, with Na^+ and Cl^- ions on either side of the bilayer. (b) System at 4 ns, where the Cl^- ion starts to drift through the pore. (c) A 6 ns snapshot showing the Cl^- ion drifting to the other side of the pore. (d) Cl^- seen to go completely to the other side of the bilayer at 7 ns, while Na^+ is at the membrane–water interface region during the entire process.

Acknowledgements

We acknowledge A. Pakhomov (ODU) for useful discussions. Partial support from Old Dominion University is gratefully acknowledged. Finally, we like to acknowledge the Texas Advanced Computing Center and Center for Computational Biology and Bioinformatics for resources in carrying out the MD simulations on multiple processors.

References

[1] R. Stampfli, Reversible electrical breakdown of the excitable membrane of a Ranvier node, An. Acad. Brasil. Ciens. 30 (1958) 57–63.
[2] E. Neumann, K. Rosenheck, Permeability changes induced by electric impulses in vesicular membranes, J. Membr. Biol. 10 (1972) 279–290.
[3] T.Y. Tsong, Electroporation of cell membranes, Biophys. J. 60 (1991) 297–306.
[4] J.C. Weaver, Y.A. Chizmadzhev, Theory of electroporation: a review, Bioelectrochem. Bioenerg. 41 (1996) 135–160.
[5] I.G. Abidor, V.B. Arakelian, Y. Chemomordik, A. Chizmadzhev, V.F. Pastushenko, M.R. Tarasevich, Electrical breakdown of bilayer lipid membranes: the main experimental facts and their qualitative discussion, Bioelectrochem. Bioenerg. 6 (1979) 37–52.
[6] G.A. Hoffmann, S.B. Dev, G.S. Nanda, Electroporation therapy: a new approach for the treatment of head and neck cancer, IEEE Trans. Biomed. Eng. 46 (1999) 752–758.
[7] D.C. Chang, B.M. Chassy, J.A. Saunders, A.E. Sowers, Guide to Electroporation and Electrofusion, Academic Press, New York, 1992.
[8] E. Neumann, A.E. Sowers, C.A. Jordan, Electroporation and Electrofusion in Cell Biology, Plenum Press, New York, 1989.
[9] S. Orlowski, L.M. Mir, Cell eletro-permeabilization: a new tool for biochemical and pharmacological studies, Biochim. Biophys. Acta 1154 (1993) 51–63.
[10] J.C. Weaver, Electroporation: a general phenomena for manipulating cells and tissues, J. Cell. Biochem. 51 (1993) 426–435.
[11] K.H. Schoenbach, R.P. Joshi, J.F. Kolb, N. Chen, M. Stacey, P.F. Blackmore, E.S. Buescher, S.J. Beebe, Ultrashort electrical pulses open a new gateway into biological cells, Proc. IEEE 92 (2004) 1122–1137.
[12] K.C. Melikov, V.A. Frolov, A. Shcherbakov, A.V. Samsonov, Y.A. Chizmadzhev, L.V. Chernomordik, Voltage-induced nonconductive pre-pores and metastable single pores in unmodified planar lipid bilayer, Biophys. J. 80 (2001) 1829–1836.
[13] V. Zlatko, A.T. Esser, T.R. Gowrishankar, J.C. Weaver, Membrane electroporation: the absolute rate equation and nanosecond time scale pore creation, Phys. Rev. E. 74 (2006) 021904/1–021904/12.
[14] N. Chen, K.H. Schoenbach, J.F. Kolb, R.J. Swanson, A.L. Garner, J. Yang, R.P. Joshi, S.J. Beebe, Leukemic cell intracellular responses to nanosecond electric fields, Biochem. Biophys. Res. Commun 317 (2004) 421–427.
[15] P.T. Vernier, Y. Sun, L. Marcu, S. Salemi, C.M. Craft, M.A. Gundersen, Calcium bursts induced by nanosecond electric pulses, Biochem. Biophys. Res. Commun. 310 (2003) 286–295.
[16] S.J. Beebe, P.F. Blackmore, J. White, R.P. Joshi, K.H. Schoenbach, Nanosecond pulsed electric fields modulate cell function through intracellular signal transduction mechanisms, Physiol. Meas. 25 (2004) 1077–1093.
[17] R.P. Joshi, A. Nguyen, V. Sridhara, Q. Hu, R. Nuccitelli, K.H. Schoenbach, Simulations of intra-cellular calcium release dynamics in response to a high-intensity, ultrashort electric pulse, Phys. Rev. E. 75 (2007) 041920/1–041920/10.
[18] K.H. Schoenbach, R.P. Joshi, R.H. Stark, F.C. Dobbs, S.J. Beebe, Bacterial decontamination of liquids with pulsed electric fields, IEEE Trans. Dielectr. Electr. Insul. 7 (2000) 637–645.

[19] R. Nuccitelli, U. Pliquett, X. Chen, W. Ford, J.R. Swanson, S.J. Beebe, J.F. Kolb, K.H. Schoenbach, Nanosecond pulsed electric fields cause melanomas to self-destruct, Biochem. Biophys. Res. Commun. 343 (2006) 351–360.
[20] M. Stacey, J. Stickley, P. Fox, V. Statler, K.H. Schoenbach, S.J. Beebe, S. Buescher, Differential effects in cells exposed to ultra-short, high intensity electric fields: cell survival, DNA damage, and cell cycle analysis, Mutat. Res. 542 (2003) 65–75.
[21] J.C. Neu, W. Krassowska, Modeling postshock evolution of large electropores, Phys. Rev. E Stat. Nonlinear Soft Matter Phys. 67 (2003) 021915/1–021915/12.
[22] R.P. Joshi, Q. Hu, K.H. Schoenbach, Dynamical modeling of cellular response to short-duration, high-intensity electric fields, IEEE Trans. Dielectr. Electr. Insul. 10 (2003) 778–787.
[23] Q. Hu, R.P. Joshi, K.H. Schoenbach, Simulations of nanopore formation and phosphatidylserine externalization in lipid membranes subjected to a high-intensity, ultrashort electric pulse, Phys. Rev. E Stat. Nonlinear Soft Matter Phys. 72 (2005) 031902/1–031902/10.
[24] Q. Hu, S. Viswanadham, R.P. Joshi, K.H. Schoenbach, S.J. Beebe, P.F. Blackmore, Simulations of transient membrane behavior in cells subjected to a high-intensity ultrashort electric pulse, Phys. Rev. E Stat. Nonlinear Soft Matter Phys. 71 (2005) 031914/1–031914/10.
[25] D.P. Tieleman, H. Leontiadou, A.E. Mark, S.J. Marrink, Simulation of pore formation in lipid bilayers by mechanical stress and electric fields, J. Am. Chem. Soc. 125 (2003) 6382–6383.
[26] E. Neumann, Membrane electroporation and direct gene transfer, Bioelectrochem. Bioenerg. 28 (1992) 247–267.
[27] V.L. Sukhorukov, H. Mussauer, U. Zimmermann, The effect of electrical deformation forces on the electropermeabilization of erythrocyte membranes in low- and high-conductivity media, J. Membr. Biol. 163 (1998) 235–245.
[28] G. Pucihar, T. Kotnik, M. Kanduser, D. Miklavcic, The influence of medium conductivity on electropermeabilization and survival of cells in vitro, Bioelectrochemistry 54 (2001) 107–115.
[29] E. Ferreira, E. Potier, D. Logeart-Avramoglou, S. Salomskaite-Davalgiene, L.M. Mir, H. Petite, Optimization of a gene transfer method for mesenchymal stem cell transfection, Gene Ther. 15 (2008) 537–544.
[30] Y. Antov, A. Barbul, H. Mantsur, R. Korenstein, Electroendocytosis: exposure of cells to pulsed low electric fields enhances adsorption and uptake of macromolecules, Biophys. J. 88 (2005) 2206–2223.
[31] T. Kotnik, F. Bobanovic´, D. Miklavcic, 285–291, Sensitivity of transmembrane voltage induced by applied electric fields—a theoretical analysis, Bioelectrochem. Bioenerg. 43 (1997) 285–291.
[32] M.P. Rols, J. Teissie, Ionic-strength modulation of electrically induced permeabilization and associated fusion of mammalian cells, Eur. J. Biochem. 179 (1989) 109–115.
[33] A. Ivorra, J. Villemejane, L.M. Mir, Electrical modeling of the influence of medium conductivity on electroporation, Phys. Chem. Chem. Phys. 12 (2010) 10055–10064.
[34] D.O.H. Suzuki, A. Ramos, M.C.M. Ribeiro, L.H. Cazarolli, F.R.M.B. Silva, L.D. Leite, J.L.B. Marques, Theoretical and experimental analysis of electroporated membrane conductance in cell suspension, IEEE Trans. Biomed. Eng. 58 (2011) 3310–3318.
[35] J. Li, W. Tan, M. Yu, H. Lin, The effect of extracellular conductivity on electroporation-mediated molecular delivery, Biochim. Biophys. Acta 1828 (2013) 461–470.
[36] A.A. Gurtovenko, I. Vattulainen, Ion leakage through transient water pores in protein-free lipid membranes driven by transmembrane ionic charge imbalance, Biophys. J. 92 (2007) 1878–1890.
[37] W. Frey, J.A. White, R.O. Price, P.F. Blackmore, R.P. Joshi, R. Nuccitelli, S.J. Beebe, K.H. Schoenbach, J.F. Kolb, Transmembrane voltage changes during nanosecond pulsed electric exposure, Biophys. J. 90 (2006) 3608–3615.
[38] M. Pavlin, M. Kanduser, M. Rebersek, G. Pucihar, F. Hart, R. Magjarevic, D. Miklavcic, Effect of cell electroporation on the conductivity of a cell suspension, Biophys. J. 88 (2005) 4378–4390.
[39] H.Y. Wang, C. Lu, High-throughput and real-time study of single cell electroporation using microfluidics: effects of medium osmolarity, Biotechnol. Bioeng. 95 (2006) 1116–1125.
[40] A.G. Pakhomov, A.M. Bowman, B.L. Ibey, F.M. Andre, O.N. Pakhomova, K.H. Schoenbach, Lipid nanopores can form a stable, ion channel-like conduction pathway in cell membrane, Biochem. Biophys. Res. Commun. 385 (2009) 181–186.
[41] H.J.C. Berendsen, D. van der Spoel, R. van Drunen, GROMACS: a message-passing parallel molecular dynamics implementation, Comput. Phys. Commun. 95 (1995) 43–56.
[42] O. Berger, O. Edholm, F. Jahnig, Molecular dynamics simulations of a fluid bilayer of dipalmitoylphosphatidylcholine at full hydration, constant pressure, and constant temperature, Biophys. J. 72 (1997) 2002–2013.
[43] H.J.C. Berendsen, J.P.M. Postma, W.F. van Gunsteren, A. DiNola, J.R. Haak, Molecular dynamics with coupling to an external bath, J. Chem. Phys. 81 (1984) 3684–3690.
[44] S. Mabrey, J.M. Sturtevant, Proc. Natl. Acad. Sci. U. S. A. 73 (1976) 3862.
[45] C.H. Huang, J.R. Lapides, I.W. Levin, J. Am. Chem. Soc. 104 (1982) 5926.
[46] S.J. Marrink, J. Risselada, A.E. Mark, Chem. Phys. Lipids 135 (2005) 223.
[47] M.J. Ziegler, P.T. Vernier, J. Phys. Chem. B 112 (2008) 13588–13596.
[48] T. Darden, D. York, L. Pedersen, Particle mesh Ewald: an $N\cdot\log(N)$ method for Ewald sums in large systems, J. Chem. Phys. 98 (1993) 10089–10092.
[49] B. Hess, H. Bekker, H.J. Berendsen, LINCS: a linear constraint solver for molecular simulations, J. Comput. Chem. 18 (1997) 1463–1472.
[50] http://www.ks.uiuc.edu/Research/vmd/ .
[51] S.A. Pandit, D. Bostick, M.L. Berkowitz, Molecular dynamics simulation of a dipalmitoylphosphatidylcholine bilayer with NaCl, Biophys. J. 84 (2003) 3743–3750.
[52] R.A. Bockmann, A. Hac, T. Heimburg, H. Brubmuller, Effect of sodium chloride on a lipid bilayer, Biophys. J. 85 (2003) 1647–1655.
[53] M. Yu, H. Lin, Quantification of propidium iodide delivery with millisecond electric pulses: a model study, http://arxiv.org/abs/1401.6954 Jan. 28, 2014.
[54] A. Polak, D. Bonhenry, F. Dehez, P. Kramar, D. Miklavcic, M. Tarek, On the electroporation thresholds of lipid bilayers: molecular dynamics simulation investigations, J. Membr. Biol. 246 (2013) 843–850.